Novel compound waste heat-solar driven ejector-compression heat pump for simultaneous cooling and heating using environmentally friendly refrigerants

Ali Khalid Shaker Al-Sayyab[a,b,*], Adrián Mota-Babiloni[a], Joaquín Navarro-Esbrí[a]

[a] ISTENER Research Group, Department of Mechanical Engineering and Construction, Universitat Jaume I, Campus de Riu Sec s/n, 12071 Castelló de la Plana, Spain

[b] Basra Engineering Technical College (BETC), Southern Technical University, Basra, Iraq

Abstract

This work investigates the theoretical performance of a novel compound waste heat-solar driven ejector-solar assisted heat pump for simultaneous heating and cooling purposes. The system utilizes waste heat from three different sources, PV/T (photovoltaic thermal) with flat plate collector, milk pasteurization process, and condenser exchange heat. Real weather data is employed to determine the hourly performance of the system in three European cities, Valencia (Spain), Berlin (Germany), and Stockholm (Sweden) representing warm, middle and cold climates, respectively. Moreover, R450A and R513A alternative refrigerants are compared to the greenhouse gas R134a. The results show that the proposed system improves cooling COP by 7% using R450A in comparison with a conventional R134a vapor compression system. Furthermore, the utilization of waste heat recovery enhances the system COP from 3.7 to 4 in the absence of solar intensity. On the other hand, the results of the heating mode show that the system with PV/T and using R450A has a COP increase over the adopted solar time, ranging from 2 to 5% in Valencia; 2 to 2.5% in Berlin, and1 to 1.5% in Stockholm. However, R513A shows a COP reduction of about 5% in comparison to R134a. Regarding the heating mode with waste heat utilization from milk pasteurization, the system based on R450A results in the highest system COP, increasing COP up to 75% compared to the R134a baseline scenario. Overall, the proposed R450A systems show the highest equivalent carbon dioxide emission reduction and, therefore, it is recommended from an environmental point of view.

Keywords: waste heat recovery; PV/T; low global warming potential (GWP) refrigerants; solar ejector; vapor compression.

Highlights

- A novel compound waste heat-solar driven ejector-solar assisted heat pump is proposed.
- Environmentally friendly refrigerants are studied as alternatives to R134a.
- The system utilizes heat from flat plate collector PV/T, milk pasteurization, and condenser.
- Waste heat recovery enhances the system COP in the absence of solar intensity.
- R450A improves system COP in most of scenarios.

[*] *Corresponding author*: Ali Khalid Shaker Al-Sayyab
E-mail: alsayyab@uji.es, ali.alsayyab@stu.edu.iq

Nomenclature

A	Area (m^2)
C	Refrigerant velocity ($m.s^{-1}$)
COP	Coefficient of performance (-)
EC	Energy consumption ($kWh.year^{-1}$)
h	Specific enthalpy ($kJ.kg^{-1}$)
I	Solar intensity ($W.m^{-2}$)
LK	Refrigerant system annual leakage rate (kg)
M	Mach number (-)
NBP	Normal boiling point (°C)
P	Pressure (MPa)
RT	Running time of the system (hour)
rpm	Revolution per minute
T	Temperature (°C)
V	Volume (m^3)
$\dot{m}$	Refrigerant mass flow rate ($kg.s^{-1}$)
$\dot{Q}$	Heat transfer rate (kW)
$\dot{W}$	Electrical consumption power (kW)

Greek symbols

α	Life of the system (year)
β	Carbon emission factor (CO_2-$eq.kWh^{-1}$)
ε	Heat exchanger effectiveness (-)
ρ	Refrigerant density ($kg.m^{-3}$)
η	Efficiency (-)
γ	Adiabatic index (-)

Subscripts

C	Compressor
Cri	Critical condition
D	Diffuser
DS	Displacement
e	Evaporator
em	Electrical mechanical
h	Hot stream; heating mode
HX	Heat exchanger
in	Inlet
int	Intermediate conditions
k	Condenser
l	Cold stream; cooling mode
m	Mixing conditions
n	Normal shock conditions
out	Outlet
P	Pump
P,i	Pump inlet
pn	Primary nozzle
P,o	Pump outlet
r	Ratio

sn	Suction nozzle
t	Total
v	Volumetric
i	After expansion condition
fg	vaporization

Abbreviatures

CO_2-eq	Equivalent carbon dioxide emissions
EES	Engineering Equation Solver
GWP	Global warming potential
HFC	Hydrofluorocarbon
HP	Heat pump
ODP	Ozone depletion potential
PCM	Phase change material
PV/T	Photovoltaic thermal
RMSD	Root-mean-square deviation
SAHP	Solar assisted heat pump
SDEC	Solar driven ejector compression system
TEWI	Total Equivalent Warming Impact
BV	Bypass valve
MECR	Modified ejection-compression refrigeration cycle

1. Introduction

Population density increases and life evolution produces steadily increasing environmental pollution with growing global energy demands. All of these factors require finding competitive and environmental-friendly alternative energy sources. Energy efficiency enhancement is the most cost-effective and competitive way to reduce CO_2-eq emissions, improve energy security, and make energy more affordable for consumers [1].

In March 2007, the European Council announced the initiative '20/20/20 targets', setting three ambitious targets: 20% energy efficiency increase, 20% greenhouse gases emissions reduction, and 20% renewable energy dependence increase [1]. On 15 October 2016, the meeting parties of the Montreal-Protocol agreed to add HFCs to the list of controlled substances and approved a timeline for their gradual reduction by 80-85% by late 2040 [2]. R134a is still one of the most used HFCs in refrigeration and air conditioning applications, and because of its high global warming potential (GWP) value, it should be phased out.

Solar energy is clean, readily available, and renewable, and has received much attention in recent years due to the growing global energy needs and concern for environmental degradation. The thermal heat collected from solar energy usually has a moderate temperature, which cannot be used directly for heating. Nevertheless, it can be used as a heat source for heat pumps, by coupling a flat plate collector or Photovoltaic/Thermal (PV/T). This system, named solar assisted heat pump, absorbs less electric power in comparison to conventional heat pumps. It can operate at higher evaporating temperatures than conventional systems, which are based on fan-coil evaporators at temperatures 5-15 °C below ambient [3].

Up to date, a few studies assessed the improvement of the heat pump system efficiency and by using flat plate collectors as a heat source for direct expansion heat pumps. Moreno-Rodríguez et al. [4] developed

and validated a theoretical model that showed that the highest coefficient of performance (COP) results in warmer climates. Liu et al. [5] compared this system with a 160 kW gas-boiler for space heating at cold climatic conditions. The solar-assisted system satisfied the heating demand with a 55% energy-saving. Paradeshi et al. [6], using R22 and a glazed type flat-plate solar collector, concluded that the increase of solar intensity, ambient air temperature, and collector area has a notable influence on system COP.

Then, some authors have carried out simulations to evaluate the performance of direct expansion solar assisted heat pumps. Deng and Yu [7] simulated combined solar/air dual-source direct-expansion solar-assisted heat pumps for domestic water heating applications with a flat-plate solar collector as the evaporator. At low solar radiation (100 $W.m^{-2}$), the modified system has a 14.1% higher average COP than that of the conventional system with a 19.8% decrease in heating time. Kong et al. [8] used R410A to simulate this system and obtained that the augmentation of both solar intensity and ambient temperature has a positive influence on system COP and condenser heating capacity.

Besides, other studies investigated the performance of indirect expansion solar-assisted heat pump systems with performance enhancement technics or alternative refrigerants. Cai et al. [9] considered systems composed by two solar flat-plate collectors with an aperture area of 3.2 m^2. The simulation could predict the system performance with RMSDs (root-mean-square deviation) less than 5%. Youssef et al. [10] observed that the use of a PCM (phase change material) heat exchanger has a significant influence on system stability and performance. The average COP increasing on sunny and cloudy days were 6.1% and 14.0%, respectively. Lee et al. [11] experimentally proved that a system using R1233zd(E) has a higher COP than that of R134a, but with lower heating capacity.

A few studies proved that the solar energy surplus collected by a PV/T panel and used as a heat source for the heat pump evaporator could enhance the system performance. Dott et al. [12] evaluated combinations of the solar absorber and PV/T with a heat pump for space heating and obtained that all situations enhance the seasonal performance factor. Wang et al. [13] analyzed a PV/T solar assisted heat pump(PV/T-SAHP) for cooling and heating applications. The PV/T-SAHP system presented higher exergy performance and obtained that exergy consumption per investment unit can be decreased by installing solar cells of higher heating capacity. Tsai [14] developed a PV/T solar-assisted R134a heat pump with a rated power of 1 kW that proved that the solar electricity could provide the required heat pump compressor power. Del Amo et al. [15] investigated the effect of a R134a heat pump coupled to a PV/T panels and storage tanks. This combination improved by 12.5% of the electric generated per year, with a 56% improvement in the system COP.

In the same way, the performance of combined PV/T heat pump systems can be improved by using multiple heat sources. Wang et al. [16] studied the performance of a PV/T air dual-heat-source composite heat pump with R22 as a refrigerant. The study concluded that this system provides higher performance. Qu et al. [17] evaluated a solar PV/T integrated dual-source heat pump-water heating system using R134a as a refrigerant. The results show that the hot water temperature modification has the worst effect on the system COP, whereas the variation of the evaporator water inlet temperature has a positive effect. Kim et al. [18] predicted the performance of a heat pump with several heat sources (air, ground and solar) for multiple purposes: heating, cooling and domestic hot water. The simulation shows that the consumption power with solar source was reduced between 13 and 19%, and between 1 and 3%, in comparison to those results obtained with air and ground source heat pump, respectively.

The performance of PV/T solar assisted heat pumps can be enhanced with environmentally friendly refrigerants. Bai et al. [19] presented a combined hybrid PV/T solar-assisted R410A heat pump that showed a 67% energy saving compared to a conventional heating system. Izquierdo [20] studied an experimental study for PV/T solar assisted R410A heat pumps that can reduce the CO_2-eq emissions when used instead of gas-oil and natural gas boilers. Yao et al.[21] simulated a direct expansion solar assisted heat pump with PV/T modules as evaporator coupled to a build-in PCM storage tank. The increase of solar radiation, ambient temperature, and PV/T collector area have an enhanced effect on heating COP, which can be 70% higher than that of a conventional air conditioning system.

Other studies used a modified design of a PV/T collector to enhance the thermal performance of the combined heat pump system. Zhang et al. [22] considered a solar photovoltaic/heat-pipe heat pump system for space heating or hot water generation based on R134a that improved COP. Lerch et al. [23] compared arrangements of solar energy and heat pumps. The parallel arrangement has a significant increase in system performance, reducing the total electricity consumption by 30% compared to a conventional system. Zhou et al. [24] investigated the performance of a solar-driven direct-expansion R410A heat pump at the real-time operational condition. The PV/T surface temperature is less affected by the ambient temperature, whereas it was mainly affected by solar radiation. Zhou et al. [25] integrated a roll-bond-PV/T as an evaporator. The thermal performance was affected by both weather conditions and by the heat pump condensation temperature.

The combination of heat pumps with multiple heat sources showed benefits on the system performance. Liu et al. [26] experimentally assessed a solar-assisted R22 heat pump using air and hot water as heat sources, with the increase of outdoor air and the solar water temperature has a positive influence on both heating capacity and COP. Zheng et al. [27] proved that solar assistance in ground source heat pumps coupled with an air source significantly reduces energy consumption. Qiu et al. [28] performed a thermal performance assessment for three combinations of solar assistance and heat pump for drying applications. Solar-assisted heat pump drying system has a 40.5% consumption power saving. Zhou et al. [29] experimentally investigated the performance of a hybrid space heating system, operated by a solar-heat pump operates with R22 or gas. The option based on solar energy obtained the highest COP.

Energy, exergy and financial evaluation for solar-assisted heat pump system with different arrangements can provide complete information for the development of these systems. Bellos et al. [30] concluded that for an electricity cost ranged from 0.2 to 0.23 €/kWh, 20 m^2 PV panels coupled with an air source heat pump was the most attractive financial solution. Fu et al. [31] found that solar-assisted heat pump mode have the highest system exergetic performance, whereas the system operating has more energy savings, not suitable for the case of weak solar radiation. In twenty different European cities, Bellos et al. [32], proved that a solar-assisted heat pump system has the highest COP with 35% electricity savings than conventional heat pump systems. Xu et al. [33] obtained that for R152a modified and conventional ejection-compression refrigeration cycles, the generating temperature increasing has a positive influence on COP. Also, the modified system can save more energy and has higher exergy performance than the conventional one.

Other simulation studies present the combination of the ejector-compression heat pump with solar energy as a generator heat source for individual cooling or heating purpose. Dang [34] considered a combined solar-driven R1234ze(E)-ejector R410A-vapor compression cycle, using a vacuum tube-type solar collector as a heat source for the ejector system. The solar heat input increase has a positive effect on the COP, and

the system provides energy savings of 50% in heating mode, and 20% in the cooling mode. Chen et al. [35] simulated the performance of a flat plate direct expansion solar ejector-compression heat pump for water heating applications. They observed that both solar intensity and collector area increasing has an enhanced effect on COP and heating capacity. Wang et al. [36] evaluated the performance of a solar-driven ejector-vapor compression hybrid refrigeration system with a solar collector as a generator, and R1233zd(E), R1336mzz(Z) and R245fa as the working fluids. The R1233zd(E) systems presented the highest heating COP, followed by that of R245fa. Xu et al.[37,38] concluded that an ejection-compression R600a refrigeration cycle with a flat plate collector as a heat source improves the system COP by 24% compared to a conventional vapor compression cycle.

Waste heat is unutilized heat energy presents in many forms that dissipated into the environment associated with many industrial processes, e.g. combustion, drying, heating, or cooling. The grand temperature of waste heat varies with industrial processes ranged from low grade as 30°C to high grade more than 1000°C. Accordingly, waste heat classified as low, medium and high-grade heat. The utilization of waste heat represents a significant source of energy savings for industries. The low-grade waste heat utilized in producing heating and cooling present system performance enhancement by operating at high evaporating temperature. With increase the concerns to waste heat utilization. The overall system efficiency should be improved by reducing the emission of greenhouse gases. In the vision of waste heat utilization, should not be underestimated the sector of food and drinks processing. Owing to the most considerable portion of the total industrial waste of 25% [39].

The dairy sector covers activities related to the treatment of milk for dietary use and milk-derived products and by-products. In most countries, the dairy sector is the most important sector within the food industry. Pasteurization is the primary process in the dairy sector. Through a thermal process, bacterial growth is controlled, and the shelf life of milk and milk by-products prolonged. In dairy processing, there is a potential heat disposition (waste heat) not currently used. For instance, the raw milk should be heated in the pasteurization process to 75°C and then cooled to 30-35°C for preparing it to other steps of the product (separation, curd, etc.) [40]. Many studies deal with energy consumption of dairy processing for different countries, without any attention is paid to developments of using waste heat. Based on the literature review, all systems were working only with solar energy, with extensive use of the greenhouse gas R134a.

Cooling and heating consumptions can be satisfied by the same industrial plant or even exchanged with cooling and district heating networks. These are topics currently studied in many works because it is supposed that fifth-generation cities and industries will consider this technical solution [41]. In this context, the 2050 technology roadmap, of the International Energy Agency [42], recommended designing systems with the ability to produce heating; cooling and domestic hot water simultaneously. These systems can provide electric energy saving compared to simple reversible heat pumps that provide heating and cooling separately (mono-function). The enhanced energy efficiency and higher energy savings are experimentally proved by the works of Byren et al. [43], using prototype-heat pumps operating with R407C and R290, and Dasi et al. [44], with a transcritical CO_2 ejector in a dairy industry.

In this work, we propose, simulate, and analyze a novel compound waste heat-solar driven ejector-compression heat pump for cooling and heating purposes. In cooling mode, the heat pump is powered by solar heat-driven and includes an ejector. However, for heating mode, the solar-assisted heat pump includes a flash intercooler and waste heat utilization. Environmentally friendly refrigerants R450A and R513A are

considered and compared to R134a in both space heating and cooling applications. Moreover, the influence of solar radiation is considered, including three different European cities as a reference, Valencia (Spain), Berlin (Germany), and Stockholm (Sweden). Moreover, in both scenarios, the system utilizes waste heat from three different sources: condenser waste heat recovery for systems with moderate consumption power at zero solar intensity (overcast day conditions), PV/T waste heat with flat plate collector, and finally, milk pasteurization waste heat. The model includes using real weather data to determine the hourly performance of the system in three adopted cities in different seasons (summer and winter). The models are developed in Engineering Equation Solver (EES) software. This work evaluates numerous system configurations to provide a system able to operate by moderate consumption power with enhanced COP at overcast day conditions. Then, it assesses future-proof alternative commercial refrigerants and gives a clear hourly energetic assessment under real climate conditions in different seasons of representative European cities. Finally, carbon footprint emissions savings are evaluated for the different combinations of systems, refrigerants, and locations.

The main contributions of the present work are as follows

- Proposal of a novel compound waste heat-solar driven ejector-compression heat pump for cooling and heating purposes with using low global warming alternative refrigerants to R134a.
- Waste heat utilization from three different sources PV/T flat plate, condenser waste heat and milk pasteurization process.
- Evaluation the possibility of system operation in three different weather conditions cities, with different seasons.
- Energy performance and carbon footprint comparison realized between the three proposed scenarios with a traditional heat pump.

2. System description

2.1 Configurations

The system consists of a waste heat-solar driven ejector-solar assisted heat pump for simultaneous heating and cooling purposes. It has been developed to operate in two scenarios, either cooling or heating modes, with the utilization of waste heat for system performance enhancement. Both modes include a compressor, condenser, pump, waste heat exchangers, expansion valve, flash tank, and evaporator as main components.

In cooling mode (Fig.1.a), the system also includes an ejector, an ejector pump, generator, and waste heat recovery heat exchangers. The system uses waste heat from the PV/T panel as a heat source for the generator and maximizes the PV/T power by decreasing the operating temperature. The waste heat exchanger uses the condenser waste heat to enhance the system performance and provides the ability to operate the system with enhanced COP at zero solar intensity (overcast day conditions). Both heat exchangers are actuated separately according to the lift temperature. At lift temperatures above 40°C or solar intensity below 100 $W.m^{-2}$, the second heat exchanger actuates whereas the first heat exchanger is isolated via actuating the bypass valve (BV1). Furthermore, the remaining condenser waste heat is transferred by waste heat recovery heat exchanger with brine water as transfer media to used for milk pasteurization process.

In heating mode (Fig.1.b and c), the system uses a heat exchanger between the flash tank and the condenser outlet to increase the degree of subcooling, which leads to an increase of the cooling capacity with back pressure valve for reducing the flash tank gas pressure to compressor suction pressure.

In the scenario of PV/T waste heat (Fig.1.b), the system absorbs heat from PV/T and flat plate collector as system evaporator which leads to increase the performance of PV/T by reducing the operating temperature and enhance the system performance by operating with high evaporator temperature.

In Fig.1.c scenario, the system recovers waste heat rejected from milk pasteurization process, in order to upgrade this heat to useful temperature levels, which will have enough quality to enhance the heating system performance by operating with high evaporator temperature. A waste heat recovery heat exchanger is allocated between the product cooler of dairy plant and the system evaporator, acting as a heat source for the current system evaporator, using water brine as heat transfer media. The absorbed heat is developed with the compressor to a suitable temperature level, that is used for heating purposes. Moreover, this system can use PV/T as an auxiliary evaporator in case of factory shutdown or periods with lower production.

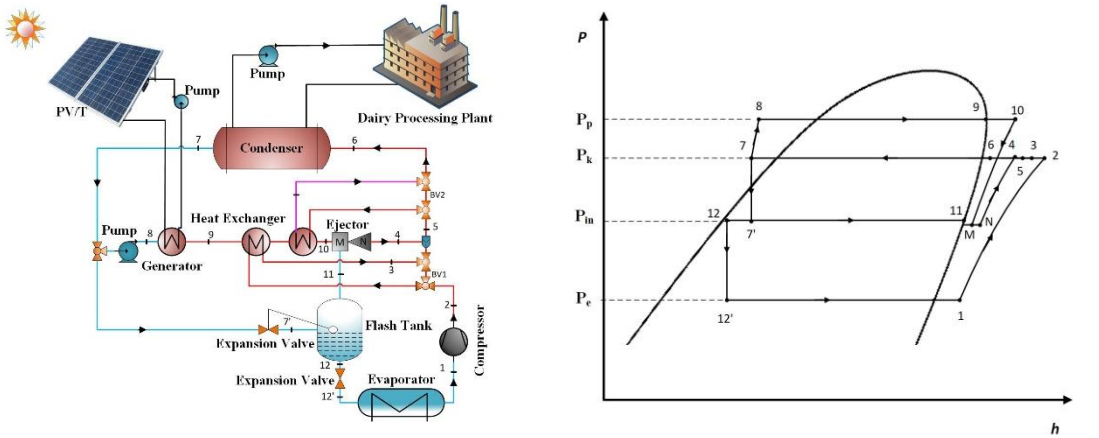

(a)

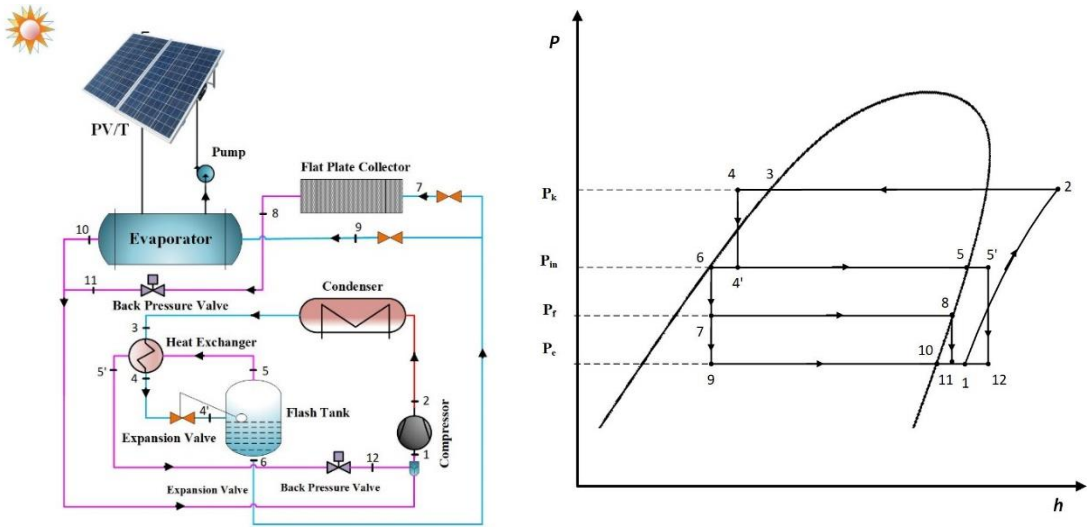

(b)

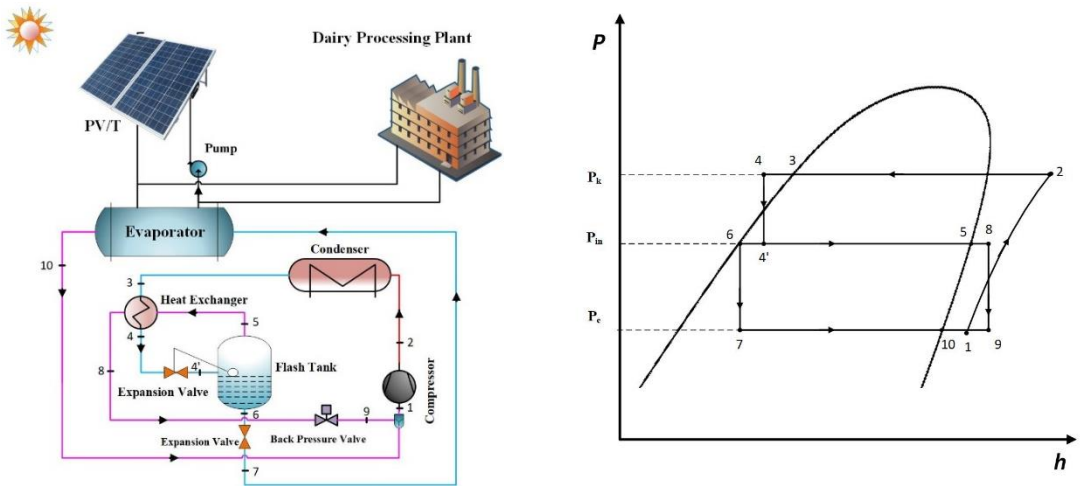

(c)

Fig.1. Schematic and P-h diagram for the proposed novel solar-driven ejector-compression system for a) cooling, b) heating mode with PV/T waste heat and c) heating mode with milk waste heat

2.2. Working fluids

HFCs are the most used fluids for replacing ozone-depleting refrigerants. Among them, R134a is used in a wide range of refrigeration and air conditioning applications, such as mobile air conditioners, domestic refrigeration, heat pumps, water chillers, etc. The utilization of R134a has increased significantly over the last ten years. However, according to Kigali Amendment to the Montreal Protocol, the production of R134a should be pended in 2050. In the current study, two environmentally friendly refrigerants, R513A and R450A are considered. Both present approximately a third of global warming potential value than R134a and has shown promising results in other applications [45]. As a drop-in replacement to R134a, both R50A and R513A show a comparable exergetic-energetic performance [46]. Moreover, both resulted in energy-savings with higher refrigeration capacity without the need for redesigning the system [47]. But if the system is adapted for R513A, the system performance could reach much higher performance than R134a [48].

Table 1 shows the main properties of the selected refrigerants and compares it to R134a. It can be seen as the proposed refrigerants has similar properties to R134a, and therefore, they can be considered as alternatives. However, the minor differences observed will produce a variation in the system operating parameters and energy efficiency. A complete assessment is required to evaluate, which is the most convenient alternative for the proposed system.

Table 1. Main properties of selected refrigerants [49,50].

Refrigerants	Molecular weight ($g.mol^{-1}$)	T_{crit} (°C)	P_{crit} (MPa)	ρ_{Vapor} [a] $kg.m^{-3}$	ρ_{liquid} [a] $kg.m^{-3}$	h_{fg} [a] $kJ.kg^{-1}$	NBP (°C)	ODP	GWP_{100}	Safety class ASHRAE
R134a	102.0	101.1	4.05	14.44	1295	198.6	-26.0	0	1430	A1
R450A	109.0	104.4	3.82	13.22	1259	185.6	-23.1	0	605	A1
R513A	108.4	96.5	3.77	17.36	1224	175.8	-29.2	0	631	A1

[a] At a temperature of 0 °C

2.3. Weather data

Household heating and cooling demand the most significant ratio of household energy consumption. In Sweden, household heating represents 35% of total electricity consumption. In Germany, building heating accounted for 41% of gas consumption. In Spanish, households heating represents 47% of total electricity consumption [51]. Given the seasonal mismatch of the European continent and to predict the current system operational feasibility over the European continent, three cities in different locations are investigated. These are Stockholm (Sweden) is selected for representing cold climate European regions, Berlin (Germany) for moderate, and Valencia (Spain) for warm locations (Table 2).

Table 2. Characteristics of selected locations [43].

City	Latitude	Longitude	Average normal solar irradiation $kWh.m^{-2}.year^{-1}$	Location
Valencia	39° 46'N	0.3763°W	1890	South
Berlin	52° 52'N	13.40° E	979	Middle
Stockholm	59° 20'N	18° E	1092	North

3. Methodology

3.1. System modelling

Fig.2 presents a schematic representation of the system strategy. EES (Engineering Equation Solver software [49] is used to model the proposed system and introduce all the considered assumptions and inputs. This software has built-in thermodynamic properties of different refrigerants and has flexibility for modelling the system components. Moreover, the model also considers equations to evaluate the system performance in different configurations, the influence of solar intensity, real climate data, and PV/T, compressor speed, and ejector sub-models.

3.2 Boundary conditions and assumptions

For the three different considering scenarios, the condensing temperature is varied from 40 to 60 ℃. In contrast, to study the effect of ambient conditions on system performance, the ambient air temperatures and hourly solar intensity of the investigated cities based on the real data of its locations[52] which will study over the solar day time which considers as input parameters. For all the operating conditions, at heating

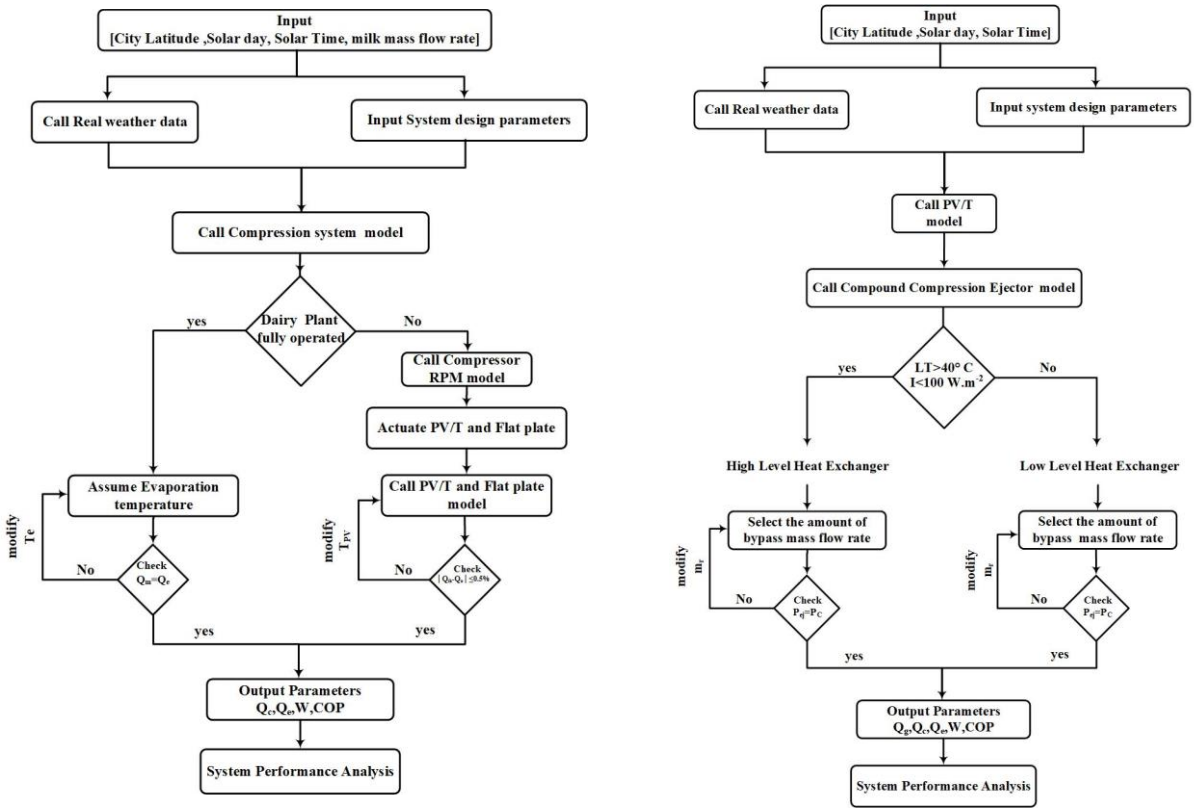

(a) (b)

Fig.2. Flow chart of system modelling a) heating mode b) cooling mode.

mode, the cooling media temperature difference across the evaporator is considered to be constant at 30 ℃, And the milk mass flow rate varied from 0.1 to 0.15 kg.s^{-1}.The refrigerant leaves the flash tank from the upper side as saturated vapor and saturated liquid from the bottom. Besides, the temperature difference between ambient air and cooling water is assumed to be 5K to reduce the heat losses from PV/T system to ambient air[53][54], the pressure drop and heat transfer to the surrounding through the connection pipes and across compressor are neglected. Table 3 contains the main assumptions and boundary conditions

Table 3. Assumptions and boundary conditions.

Parameters	Assumed value
Condensing temperature	40 to 60 °C
$\Delta T_{\text{cooling media}}$	30°C

PV/T area	1.35*0.73*3 m^2
Flat plate area	2.25*0.9*7 m^2
rpm	1500-2900
V_{DS}	0.00011 m^3
$\eta_n;\eta_{D;}\eta_{mx}$	0.8
A_m/A_{pn}	1.538 [38]
η_{em}	0.88
ε_{HX}	30%
LK	3% of refrigerant charge [55]
α	15 years
RT	Valencia: 3244 hours cooling and 3110 hours heating; Berlin: 1728 hours cooling and 4339 hours heating; and Stockholm 576 hours cooling and 5376 hours heating [52]
β	Valencia:265.4 g CO_2-eq.kWh^{-1}; Berlin:440.8 g CO_2-eq.kWh^{-1}; Stockholm:13.3 g CO_2-eq.kWh^{-1} [56]

3.3. Equations

The compressor electric consumption can be evaluated by means of Eq. (1).

$$\dot{W}_c = \eta_{em}\,\dot{m}\left(h_{c,out} - h_{c,in}\right) \tag{1}$$

The refrigerant mass flow rate delivered by the compressor is obtained by Eq. (2).

$$\dot{m} = \eta_v \rho V_{DS} rpm \tag{2}$$

The volumetric compressor efficiency is calculated by using Eq. (3) this correlation has been proposed from [57].

$$\eta_v = 0.959 - 0.00642 P_r \tag{3}$$

The heating capacity (condenser) is evaluated from Eq. (4) that considers the refrigerant specific enthalpy difference across the condenser multiplied by the refrigerant mass flow rate.

$$\dot{Q}_k = \dot{m}_k\left(h_{k,out} - h_{k,in}\right) \tag{4}$$

In the same way, the cooling capacity (evaporator) is obtained from Eq. (5).

$$\dot{Q}_e = \dot{m}\left(h_{e,in} - h_{e,out}\right) \tag{5}$$

Heat exchangers effectiveness can be obtained using Eq. (6).

$$\varepsilon_{HX} = \frac{h_{in,h} - h_{out,h}}{h_{in,h} - h_{in,l}} \tag{6}$$

The ejector operation is modelled following the work of one-dimensional analysis by Hung et al. [58]. For sonic suction nozzle, the pressure can be calculated following Eq. (7).

$$\left(\frac{p_{int}}{p_{Sn}}\right)^{\frac{\gamma}{(\gamma+1)}}=\frac{\gamma+1}{2} \tag{7}$$

The temperature of the sonic suction nozzle can be evaluated by Eq. (8).

$$\left(\frac{T_{int}}{T_{Sn}}\right)=\frac{\gamma+1}{2} \tag{8}$$

The velocity of the primary nozzle stream can be obtained as indicated in Eq. (9).

$$C_{pn}=\sqrt{2\,\eta_{pn}(h_{p,o}-h_i)} \tag{9}$$

The mixing section velocity can be obtained following Eq. (10).

$$\left(\dot{m}_{pn}C_{pn}+\dot{m}_{sn}C_{sn}\right)\eta_m=\dot{m}_{mx}C_{mx} \tag{10}$$

At mixing suction and normal shock conditions, the Mach number can be evaluated by Eq. (11).

$$M_n=\sqrt{\frac{1+\frac{\gamma-1}{2}\,M_{mx}^2}{\gamma M_{mx}^2-\frac{\gamma-1}{2}}} \tag{11}$$

The pressure and temperature at normal shock conditions can be calculated as shown in Eq. (12) to (14), respectively.

$$\frac{P_n}{P_m}=\frac{1+\gamma M_{mx}^2}{1+\gamma M_n^2} \tag{12}$$

$$\frac{T_n}{T_m}=\frac{2+(\gamma-1)M_{mx}^2}{2+(\gamma-1)M_n^2} \tag{13}$$

$$\frac{P_k}{P_n}=\left[\frac{\eta_D(1+\gamma)}{2}M_{mx}^2+1\right]^{\frac{\gamma}{\gamma-1}} \tag{14}$$

The ejector pump consumption power is obtained through Eq. (15).

$$\dot{W}_p=\dot{m}_p\left(h_{p,out}-h_{p,in}\right) \tag{15}$$

The total system power is represented by Eq. (16).

$$\dot{W}_t=\dot{W}_p+\dot{W}_c \tag{16}$$

The system coefficient of performance (COP) in cooling and heating modes results from Eq (17) and Eq. (18), respectively.

$$COP_l = \frac{\dot{Q}_e}{\dot{W}_t} \tag{17}$$

$$COP_H = \frac{\dot{Q}_k}{\dot{W}_c} \tag{18}$$

Besides the possible energetic benefits, it is essential to determine the carbon emission of the system as well. The Total Equivalent Warming Impact (TEWI) metric is used to determine the carbon footprint for the proposed systems with each alternative refrigerant. The components of TEWI are 1) direct emissions from accidental refrigerant leakages, and 2) indirect emissions from fossil fuel burning for generating the electricity. As a result, TEWI is calculated through Eq.(19) [55].

$$TEWI = (GWP \cdot LK \cdot \alpha) + (EC \cdot \beta \cdot RT) \tag{19}$$

In the case of PV/T and flat plate as heat sources of the heat pump, models mentioned in Duffie et al. [59], Zhang et al. [60], Al-Sayyab et al. [61] and Guoying et al. [53] are used to evaluate the system performance under different solar intensity and ambient temperatures.

4. Results and discussion

4.1. Cooling mode

4.1.1. Effect of solar intensity

Fig.3.a) shows the variation of consumption power over the day in the scenario of the cooling mode. As the sun rises, the consumption power gradually decreases with solar time increasing. It reaches the lowest value for the maximum solar intensity. After this moment, the consumption power increases gradually with solar time increasing, reaching its maximum at sunset.

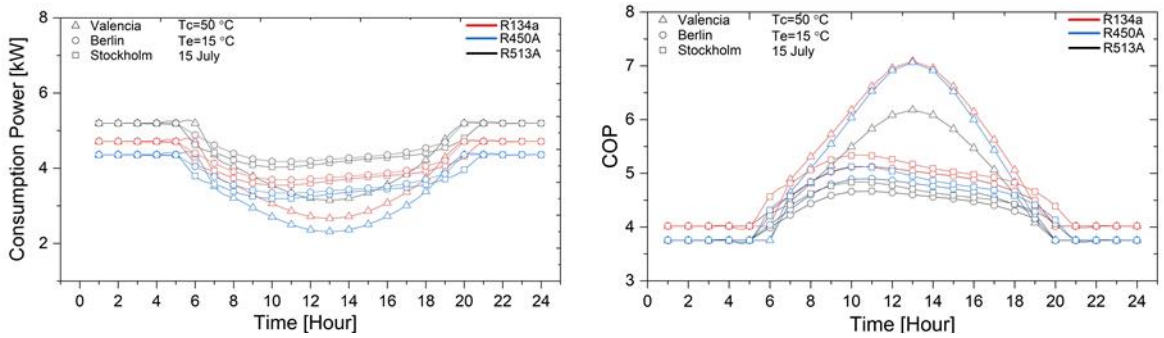

a) b)

Fig.3. Effect of solar time on a) consumption power and b) COP.

The SDEC (solar driven ejector compression) system uses waste heat from PV/T as a heat source for the generator. As a result of increasing solar intensity, the generator heat source is augmented too (Fig.4.a). This effect reduces the required pump discharge pressure (Fig.4.b), so as the pump electric consumption and system power. The system located in Valencia has the lowest consumption power because it has a higher solar intensity than Stockholm and Berlin. Fig. 4.a helps in understanding that the R450A system has the lowest consumption power compared to other investigated refrigerants. This is because it presents a low refrigerant mass flow rate, which lowers power consumption.

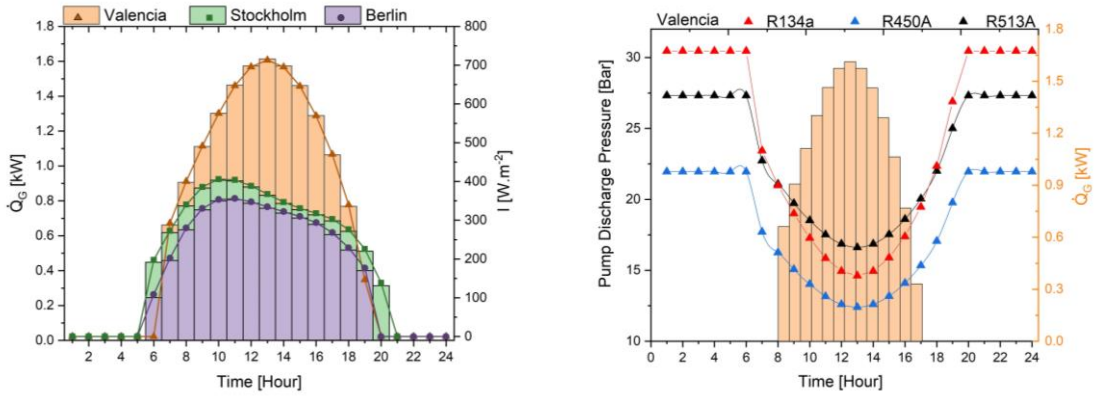

a) b)

Fig. 4. Effect of different solar time on a) Heat generated (bars) left axis and solar intensity (curves) right axis, and b) Pump discharge pressure and solar intensity.

The evolution of COP is contrary to the evolution of consumption power (Fig 3.b), so it increases gradually with solar time. It reaches the maximum value, for instance, in Valencia at 1 P.M. Moreover, the cooling capacity of the current system is not affected by solar intensity variation, operating at a constant compressor pressure ratio. Hence, the pump consumption power decreases with solar intensity and explains why in Valencia, the highest system COP is obtained. For any tested conditions, the system operated with R134a has the highest system COP, followed by R450A and R513A. R134a has the moderate cooling capacity and consumption power. At zero solar intensity, the current system provides a performance increase from 3.7 to 4, by using condenser waste heat recovery.

4.1.2. Effect of condensing temperature

The total power consumption at different condensing temperatures is presented in Fig.5.a). For all investigated locations, the tested refrigerants have similar behavior. As the condensing temperature increases, the consumption power also augments owing to the increase in pressure ratio and the required pump discharge pressure. In this case, Valencia shows the lowest power consumption overall investigated cities, influenced by the highest solar intensity. For all locations, R513A has the lowest total power consumption, followed by R134a.

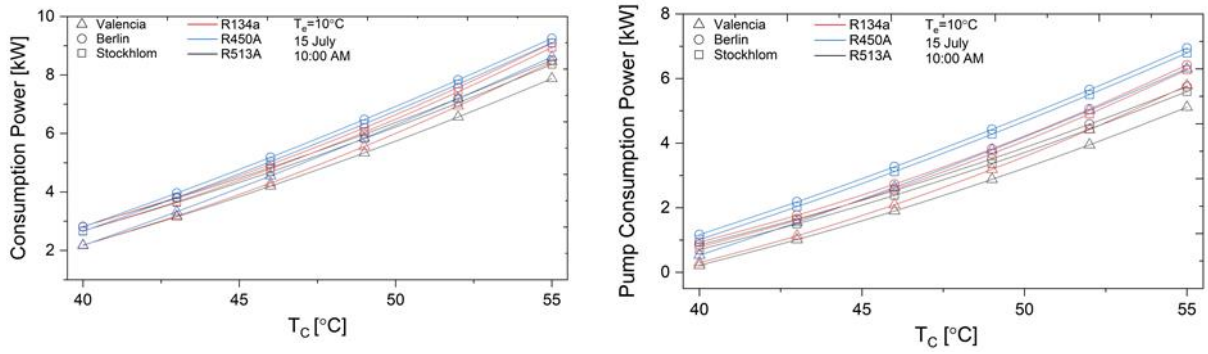

a) b)

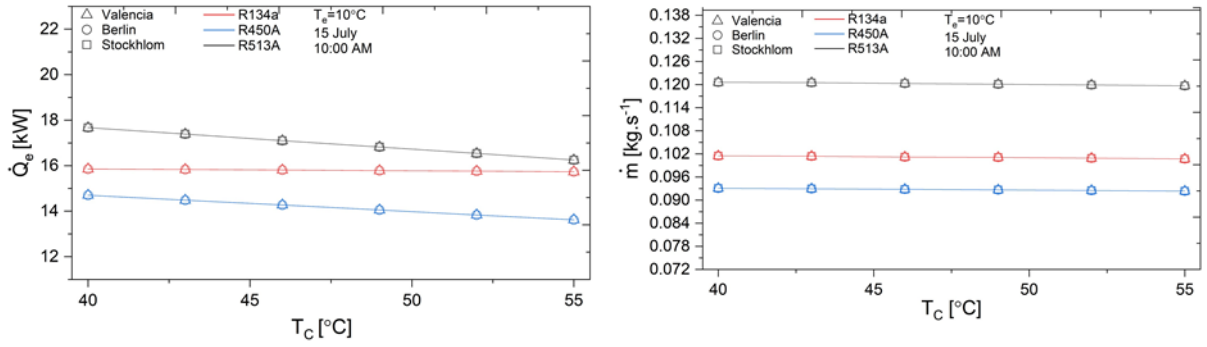

c) d)

Fig.5. Effect of condensing temperature on a) consumption power, b) pump power, c) cooling capacity, and d) refrigerant mass flow rate.

Regarding the cooling capacity, the condensing temperature slightly decreases it, due to the reduction in the latent heat of vaporization (Fig.5.c). The system using R513A has the highest cooling capacity, followed by R134a and R450A, respectively. The influence of the refrigerant mass flow rate is also presented in Fig.5.d).

As a result of condensing temperature increase, the system COP notably decreases (Fig.6) due to the increase in power consumption, and the decrease in cooling capacity. The system in Valencia has the highest COP due to the lowest operating power requirements. The system with R513A has the highest COP, with an 11% COP enhancement compared to R134a.

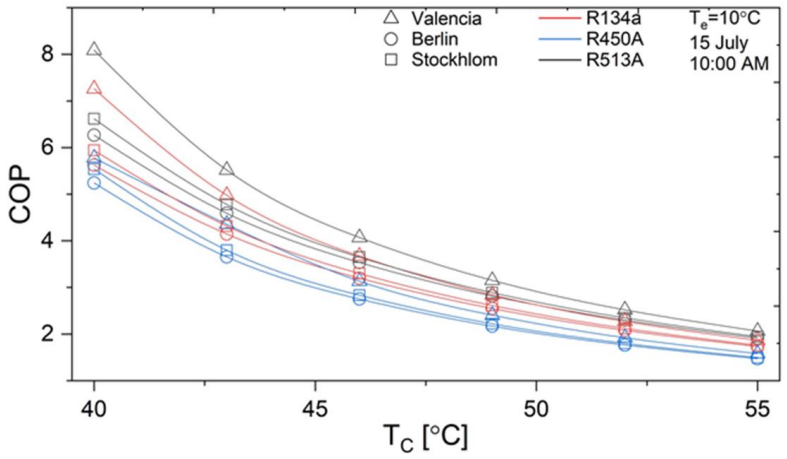

Fig.6. COP variation at different condensing temperatures.

4.2. Heating mode with PV/T waste heat

4.2.1 Effect of solar intensity

Fig.7 presents the variation of cooling capacity with solar time in January. The cooling capacity is proportional to the solar intensity, and therefore, after the sunrise, this parameter increases until reaching a maximum value around midday. The refrigerant R513A shows a slightly higher cooling capacity than R134a due to the highest refrigerant mass flow rate. However, R450A cooling capacity reduction is more

notable in Fig.7. for the same reason. The system located in Valencia city has the highest cooling capacity, owing to the highest solar intensity over the day.

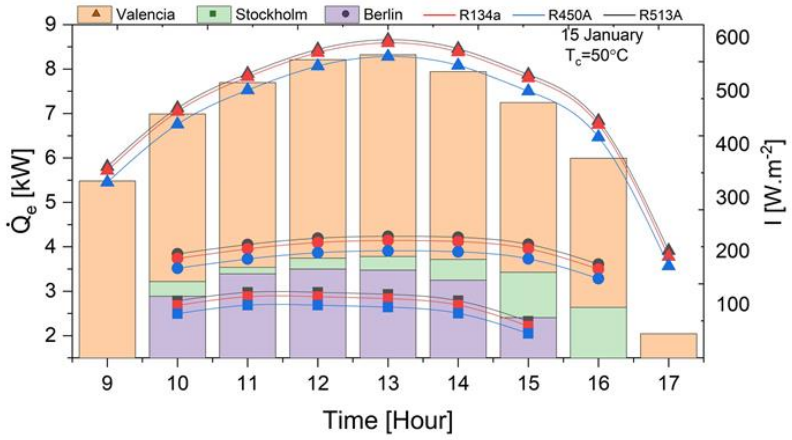

Fig.7. Cooling capacity (left axis, lines) and solar intensity (right, columns) variation at a different solar time.

Moreover, at extreme solar intensity values (overcast day condition) liquid refrigerant droplets could access to the compressor suction (in traditional thermostatic expansion valve (TEV), the turndown ratio is about 70% of maximum capacity)[62]. To prevent this situation, which can damage the compressor, relatively high-pressure ratios must be avoided, a variable speed compressor is used.

Fig.8.a) presents the power consumption along the day and shows that it increases with solar time (as the solar intensity increase) until forming a plateau at noon period. For the afternoon period, the compressor power exhibits a contrary behavior with solar time increasing. This evolution can be explained by attending to the fact that more solar energy (heat) is absorbed. Then, the evaporating temperature and pressure are increased, as observed in Fig.8.b). The condenser pressure also varies, and the compressor pressure ratio decreases, as shown in Fig.8.c).

The compressor speed needs to be augmented with the increase in solar intensity to prevent the refrigerant starving (low refrigerant mass flow rate leads to a high degree of superheating). On the other hand, to prevent evaporator overfeeding by refrigerant at low solar intensity, the contrary is occurring during the afternoon.

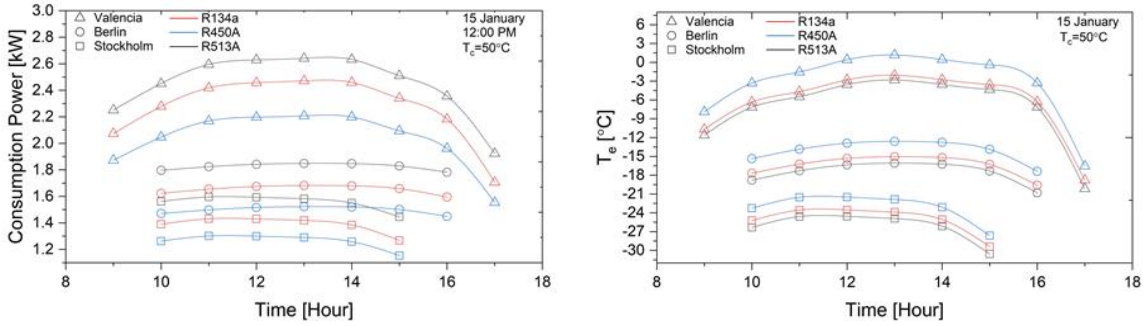

a) b)

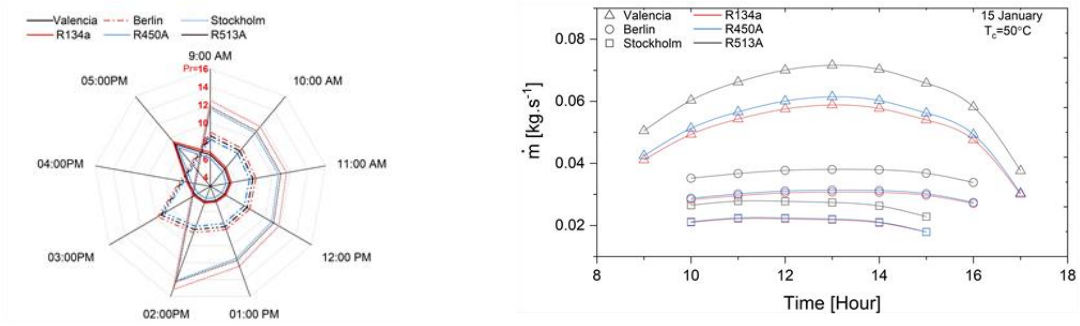

c) d)

Fig.8. Assessment of solar time variation effect on a) compressor consumption power, b) evaporator temperature, c) pressure ratio, and d) refrigerant mass flow rate.

The system in Valencia consumes more power than those systems located in the other selected cities, owing to the highest availability of solar intensity. The system using R513A requires more power than that of R134a despite presenting a lower pressure ratio, owing to a higher mass flow rate delivered (Fig.8.d). The contrary happens to the system using R450A.

Fig.9.a) illustrates the variation of heating capacity over the day. While the system located in Valencia has the highest heat delivered by the condenser, that located in Stockholm presents the lowest. Also, in this case, the heating capacity is directly proportional to solar intensity. The system with R513A results in the highest heating capacity in comparison with the other investigated refrigerants, owing to the highest refrigerant mass flow rate.

Fig.9.b) evidences that all refrigerants have similar behavior regarding system COP, which is directly proportional to solar intensity. The system located in Valencia has the highest COP in comparison to the rest of the cities, being 31% and 22% higher than Stockholm and Berlin, respectively (when the system operates with R134a). On the other hand, the alternative refrigerant R450A shows COP enhancement in all tested locations, despite it has the lowest heating capacity. However, the lowest power consumption provides an enhancement effect on system COP.

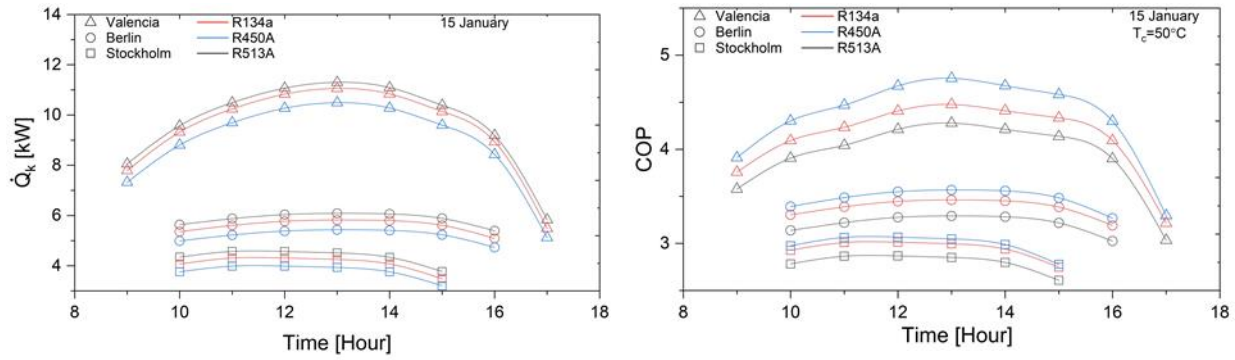

a) b)

Fig. 9. Effect of different solar time on a) heating capacity and b) system COP.

At constant condensing temperature, Fig. 10 gathers the influence on the system COP of several parameters, such as the pressure ratio, solar irradiation, and ambient air temperature. The results consider R450A as a reference, but it can be extrapolated to other refrigerants. Both solar intensity and ambient air temperature increasing have a reduction effect on compressor pressure ratio, meanwhile that have enhanced influences on system COP; this influence is notable for Valencia due to the highest solar intensity and ambient air temperature.

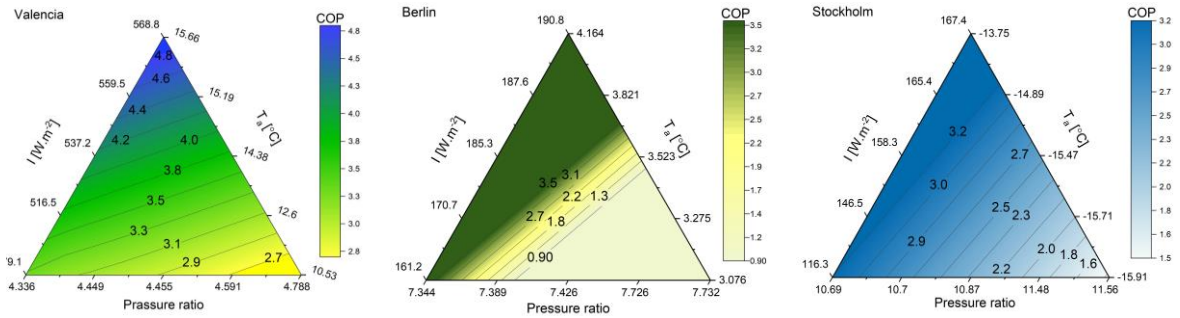

a) b) c)

Fig 10. Effect of pressure ratio, solar irradiation, and ambient air temperature on system COP in a) Valencia, b) Stockholm, and c) Berlin.

4.2.2 Effect of condensing temperature

By setting solar intensity constant at midday, the variation of condensing temperature from 40 to 60 °C has a slight influence on cooling capacity (Fig.11.a) by the decrease in the degree of subcooling. The higher mass flow rate (Fig.11.b) for R513A justifies the highest delivered cooling capacity when considering this alternative fluid.

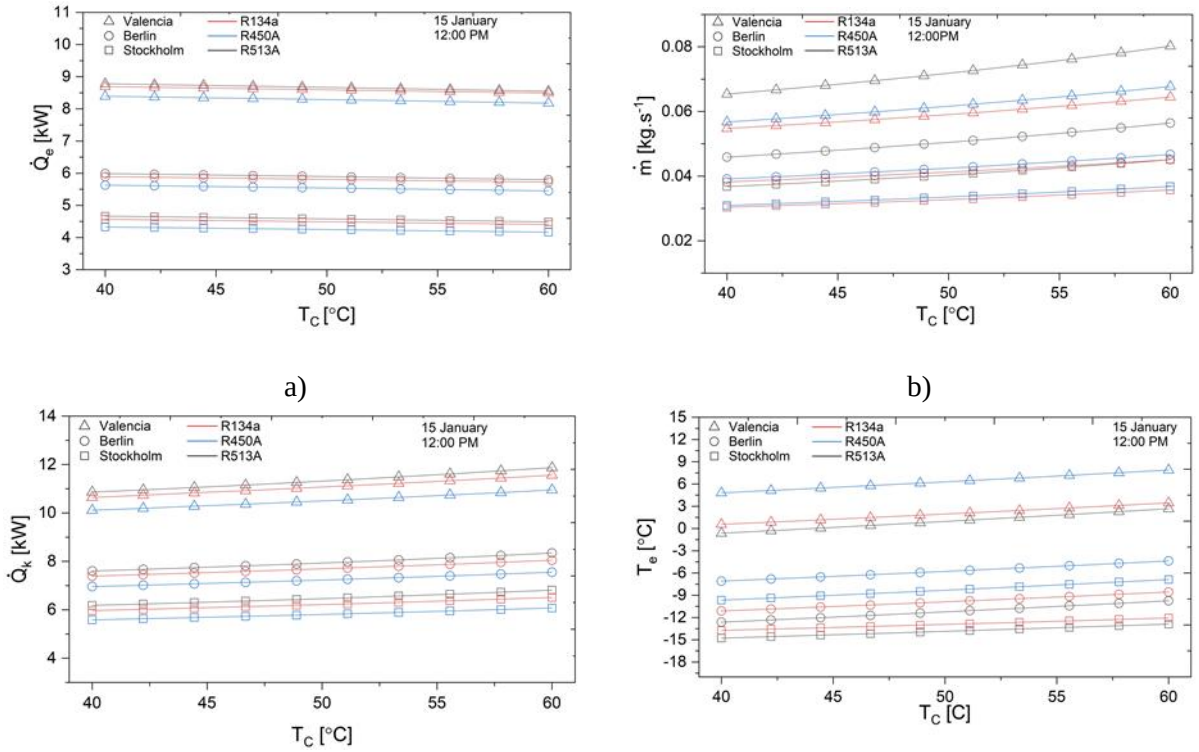

a) b)

c) d)

Fig.11. Effect of condensing temperature on a) cooling capacity, b) refrigerant mass flow rate, c) heating capacity, and d) evaporating temperature.

Similarly, the heating capacity increases slightly at a constant solar intensity and condensing temperature increasing (Fig.11.c). Meanwhile, this leads to a decrease in condenser degree of subcooling and an increase in the evaporation temperature (Fig.11.d), which has a positive effect on the refrigerant mass flow rate. The system with R513A has the highest heating capacity in comparison with other adopted refrigerants owing to the highest mass flow rate.

As illustrated in Fig.12.a), the power consumption for all investigated refrigerants is directly proportional to the condenser temperature, in compression, the system with R450A has the lowest power consumption from other refrigerants, due to moderate mass flow rate (Fig.11.b) and the lowest pressure ratio (Fig.12.b). While the system with R513A has the highest power consumption, owing to the moderate pressure ratio and the highest mass flow rate, again, the system located in the city of high solar intensity (Valencia) has the highest consumption power, due to the highest compressor speed requirement.

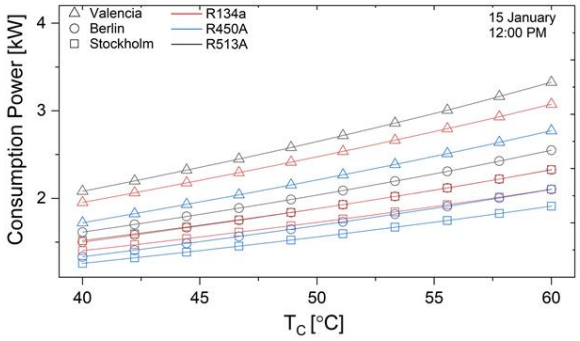

a)

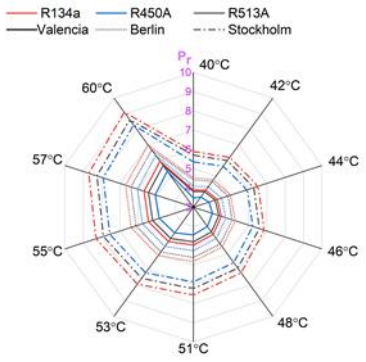

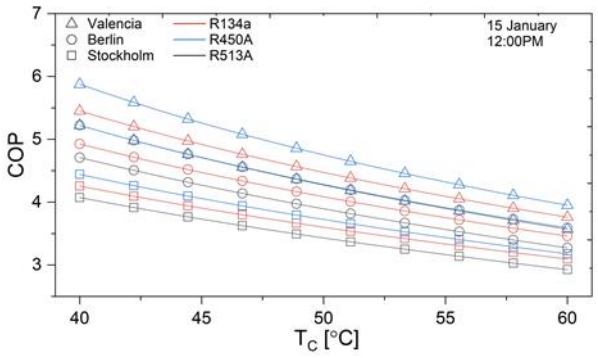

b) c)

Fig.12. Effect of condensing temperature on a) consumption power, b) refrigerant mass flow rate, c) pressure ratio and d) COP.

On the other hand, the condensing temperature increase has the worst influence on system COP that evident in Fig.12.c); also the system with refrigerant R450A has the highest system COP, while the refrigerant

R513A has the lowest in comparison with other refrigerants in spite of has the highest heating capacity, due to the highest power consumption which has an adverse effect on system COP.

Finally, Fig.13 specifies the COP improvement (or decrease) of alternative refrigerants compared to R134a. The environmentally friendly R450A shows a COP improvement over the adopted solar time of the three selected locations. It ranged from 2 to 5% in Valencia (with the more evident influence of solar intensity), 1 to 1.5% in Stockholm, and 2 to 2.5% in Berlin. Moreover, the use of R513A decreases COP in the range of 5%.

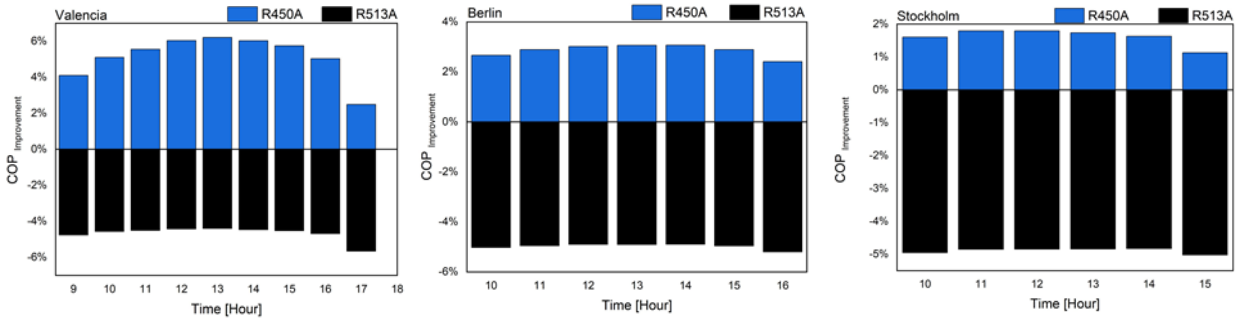

a) b) c)

Fig.13. Alternative refrigerants system COP improvement at a) Valencia, b) Berlin, and c) Stockholm.

4.3. Heating mode with milk pasteurization waste heat

The last scenario considered in this paper is the heating mode using waste heat from milk production with associated PV/T. In this case, one interaction is studied, the variation of milk mass flow rate.

Fig.14.a) presents the power consumption variation of the current system. This parameter is directly proportional to the milk mass flow rate, and therefore, if milk mass flow rate grows, also consumption power does. On the other hand, the increase of milk mass flow rate also causes a reduction in the pressure ratio (Fig.14.b). At the same time, the required refrigerant mass flow also increases, but this parameter has a significant influence on compressor power consumption. In this case, the system with R513A has the highest power consumption, followed by R134a and R450A, respectively. Also, the system located in Valencia has the highest power consumption in comparison with other tested cities, owing to the highest solar intensity.

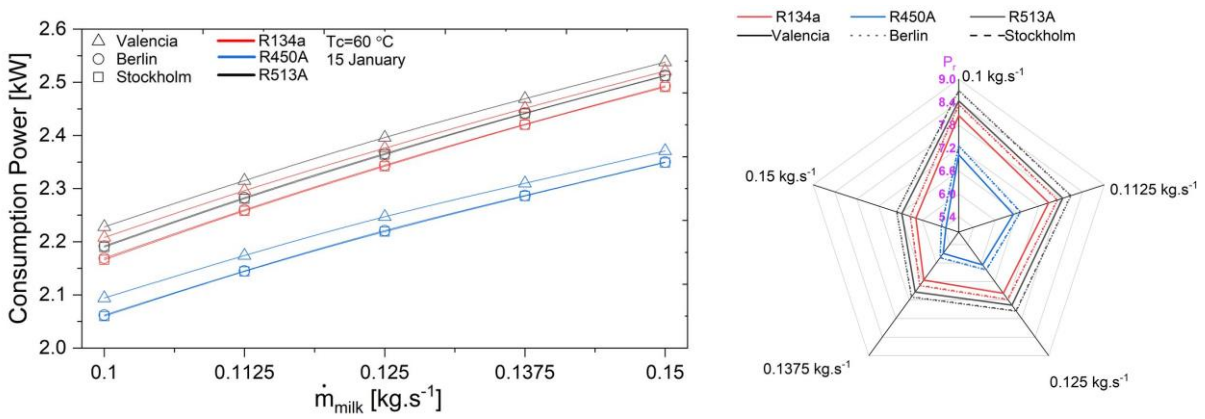

a) b)

Fig.14. Effect of milk mass flow rate on a) compressor power consumption and b) pressure ratio.

At constant solar intensity, Fig.15 clarifies the influence of milk mass flow rate and pressure ratio on different refrigerants, considering the case of Valencia as the reference. The milk mass flow rate increasing has a decreasing effect on the compressor pressure ratio of all adopted refrigerants. R450A show the lowest pressure ratio in comparison with other refrigerants (Fig.15.b). The heating capacity increases with the milk mass flow rate increasing because of pressure ratio decreasing and refrigerant mass flow rate increases both have a positive effect on the heating capacity, as depicted by Fig.15. The system with R513A has the highest heating capacity in comparison with other adopted refrigerants (owing to the lowest latent heat of vaporization which increases the degree of superheat), followed by R134a and R450A, respectively.

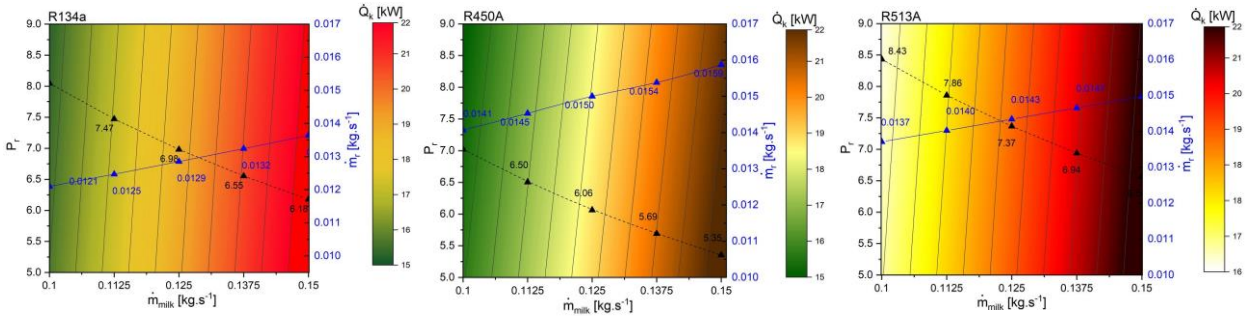

a) b) c)

Fig.15. Effect of milk mass flow rate and pressure ratio on refrigerant mass flow rate and heating capacity in Valencia for a) R134a, b) R450A, and c) R513A.

From Fig.16.a, it is evident that all adopted refrigerants have similar behavior, which is directly proportional to the milk mass flow rate. The milk mass flow rate augmentation has a notable influence on system COP. It is observed that for all tested refrigerants, the system located in Valencia has the highest system COP. Meanwhile, the system with R450A shows system COP enhancement in all tested locations from the reference case, owing to the lowest consumption power.

On the other hand, in comparison to a conventional heat pump system, the system in the current scenario with using low global warming potential refrigerants have enhanced system COP (Fig.16.b). System COP

increase ranges from 40% to 75% in the case of R450A, whereas it varies from 33% to 65% for the other alternative, R513A.

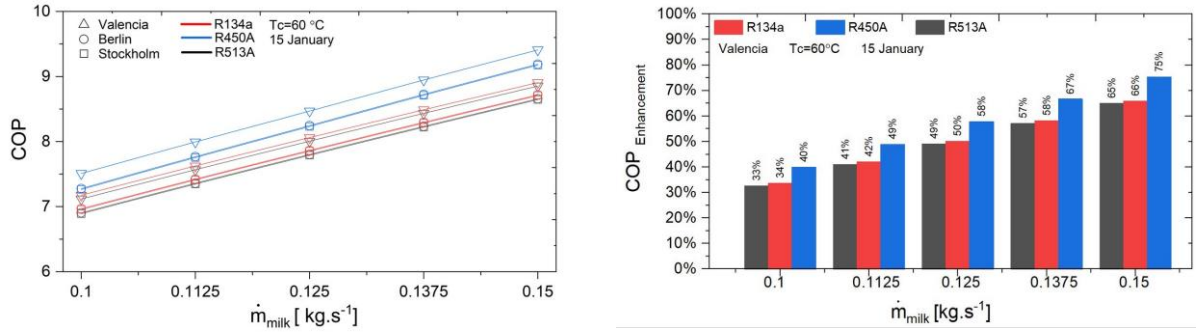

a) b)

Fig.16. Effect of milk mass flow rate variation on a) system COP, and b) COP enhancement.

4.4. Environmental comparison with conventional heat pump

As it has been proved in previous sections, the proposed system shows a system COP enhancement in all representative locations. Moreover, the utilization of environmentally friendly alternatives decreases direct CO_2-eq emission due to lower GWP values in comparison with HFCs. Therefore, the combination of both factors can result in significant carbon footprint reductions, and TEWI metric has highlighted as an accurate metric for comparing different scenarios [63]. For this simulation, a match in cooling or heating capacity with the reference has been assumed. Then, other assumptions are mentioned in table 3.

Fig.17.a) shows the TEWI reduction of the proposed system in cooling mode and an R134a conventional air conditioning (AC) unit taken as a reference for the summer season. The proposed system shows a diminution of CO_2-eq emissions with environmentally friendly refrigerants; being the system with R450A the one with the lowest emissions. Meanwhile, for all selected refrigerants, the proposed system in Stockholm shows the highest TEWI reduction than other representative cities, owing to the lowest consumption power, besides of the short period required for system operations, in comparison with other locations.

Fig.17.b) and Fig.17.c) illustrate TEWI reduction for heating mode with PV/T waste heat and milk pasteurization waste heat, respectively, taking an R134a conventional heat pump as a reference. For both scenarios, the proposed system with R450A obtained the highest TEWI reduction again, due to the combination of a low GWP value and the lowest consumption power (highest COP). The carbon emission reduction is higher in the case of milk pasteurization waste heat, considering the heat capacity match. Then, the highest evaporating load leads to an increase in the evaporating temperature (and pressure). This causes decreases the required compressor work with a positive influence on condensing heat capacity. Apart from that, the conventional heat pump based on fan coil evaporator operates between 5 and 15 °C below ambient air, explaining why Berlin has the highest TEWI reduction in case of milk pasteurization.

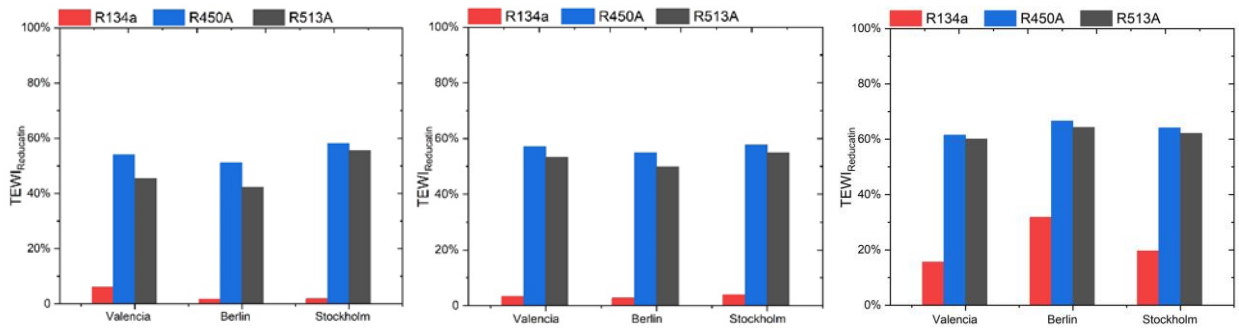

a) b) c)

Fig.17. TEWI reduction of the proposed systems with conventional R134a vapor compression system: a) cooling mode, and heating mode with b) PV/T waste heat, and c) milk pasteurization waste heat.

5. Conclusions

In this work, we provide a novel system arrangement for cooling and heating purpose with waste heat utilization by two scenarios from PV/T panels associated with using a waste heat recovery by a heat exchanger, with enhancing the system performance and with increasing the ability of operates the system with moderate consumption power at zero solar intensity (overcast day conditions). Another scenario of heating mode is by using waste heat from milk production of the dairy processing plant with associated PV/T.

For the cooling mode, the application of heat exchanger waste heat recovery enhances the system COP from 3.7 to 4 at overcast day conditions and evening conditions. At noon conditions and using R134a, the system that operates at the city of high solar intensity (Valencia) has increased COP by 41 to 43% in comparison with Berlin and Stockholm, respectively. Then, this novel system arrangement using R450A improves COP by 7% in comparison with conventional heat pump systems operates with R134a but required more heat to enhance its performance in comparison to other refrigerants.

For heating mode, in the scenario of PV/T and flat plate, the system with R450A shows a COP improvement over the adopted solar time of three different locations ranged from 2 to 5% in Valencia; 1 to 1.5% in Stockholm and 2 to 2.5% in Berlin. Also, R513A shows a COP reduction in the range of 5% in comparison to R134a. On the other hand, the solar intensity has a positive influence on cooling capacity, and R513A shows the highest heating capacity, followed by R134a and R450A, respectively.

In a scenario of waste heat from milk production, the increase of the value of milk mass flow rate has enhanced influence on system COP. In comparison to a conventional heat pump with R134a, the system using R450A presents the highest system COP, with COP increasing by 75% at a milk mass flow rate of 0.15 $kg.s^{-1}$.

All evaluated systems show a marked reduction in carbon dioxide emissions. The most significant environmental benefits are obtained when using R450A for heating mode with milk pasteurization waste heat, in which the system decreases by 61.5% the CO_2-eq emissions in Valencia, 66.5% in Berlin and 64% in Stockholm when compared with an R134a conventional heat pump.

This work has shown an example of a combination of different technologies to obtain a highly energy-efficient system. Firstly, PV/T panels can be installed in a wide range of applications, as one of the most widespread and scalable renewable energy sources. Secondly, we selected a flat plate collector and a dairy processing plant as successful cases in which this complex configuration could be considered. However, any other industry with comparable thermal requirements could be adapted to the proposed system

configuration and observe energy benefits, being able to apply most of the conclusions drawn by this paper. Moreover, there are several ways to extend conclusions reached by this paper, such as an exergoeconomic analysis for a better understanding of the benefits of the proposed system, optimizing the system components to minimize the exergy destruction, or extending the analysis to more refrigerants with global warming potential below 150.

Acknowledgements

Ali Khalid Shaker Al-Sayyab gratefully acknowledges the Southern Technical University in Iraq for the financial support to complete this work. Adrián Mota Babiloni acknowledges Generalitat Valenciana for the postdoctoral contract (APOSTD/2020/032).

References

[1] E. Implementation, European Implementation Assessment STUDY, 2016.

[2] UNEP, The Kigali Amendment to the Montreal Protocol: HFC Phase-down, OzonAction Fact Sheet. (2016) 1–7.

[3] G. Mitsopoulos, E. Syngounas, D. Tsimpoukis, E. Bellos, C. Tzivanidis, S. Anagnostatos, Annual performance of a supermarket refrigeration system using different configurations with CO2 refrigerant, Energy Convers. Manag. X. 1 (2019) 100006. doi:10.1016/j.ecmx.2019.100006.

[4] A. Moreno-Rodríguez, A. González-Gil, M. Izquierdo, N. Garcia-Hernando, Theoretical model and experimental validation of a direct-expansion solar assisted heat pump for domestic hot water applications, Energy. 45 (2012) 704–715. doi:10.1016/j.energy.2012.07.021.

[5] H. Liu, Y. Jiang, Y. Yao, The field test and optimization of a solar assisted heat pump system for space heating in extremely cold area, Sustain. Cities Soc. 13 (2014) 97–104. doi:10.1016/j.scs.2014.05.002.

[6] L. Paradeshi, M. Srinivas, S. Jayaraj, Parametric Studies of a Simple Direct Expansion Solar Assisted Heat Pump Operating in a Hot and Humid Environment, Energy Procedia. 90 (2016) 635–644. doi:10.1016/j.egypro.2016.11.232.

[7] W. Deng, J. Yu, Simulation analysis on dynamic performance of a combined solar/air dual source heat pump water heater, Energy Convers. Manag. 120 (2016) 378–387. doi:10.1016/j.enconman.2016.04.102.

[8] X.Q. Kong, Y. Li, L. Lin, Y.G. Yang, Modeling evaluation of a direct-expansion solarassisted heat pump water heater using R410A, Int. J. Refrig. 76 (2017) 136–146. doi:10.1016/j.ijrefrig.2017.01.020.

[9] J. Cai, J. Ji, Y. Wang, W. Huang, Numerical simulation and experimental validation of indirect expansion solar-assisted multi-functional heat pump, Renew. Energy. 93 (2016) 280–290. doi:10.1016/j.renene.2016.02.082.

[10] W. Youssef, Y.T. Ge, S.A. Tassou, Effects of latent heat storage and controls on stability and performance of a solar assisted heat pump system for domestic hot water production, Sol. Energy. 150 (2017) 394–407. doi:10.1016/j.solener.2017.04.065.

[11] S.J. Lee, B.H. Shon, C.W. Jung, Y.T. Kang, A novel type solar assisted heat pump using a low GWP refrigerant (R-1233zd(E)) with the flexible solar collector, Energy. 149 (2018) 386–396. doi:10.1016/j.energy.2018.02.018.

[12] R. Dott, A. Genkinger, T. Afjei, System evaluation of combined solar & heat pump systems, Energy Procedia. 30 (2012) 562–570. doi:10.1016/j.egypro.2012.11.066.

[13] C. Wang, G. Gong, H. Su, C. Wah Yu, Efficacy of integrated photovoltaics-air source heat pump systems for application in Central-South China, Renew. Sustain. Energy Rev. 49 (2015) 1190–1197. doi:10.1016/j.rser.2015.04.172.

[14] H.L. Tsai, Modeling and validation of refrigerant-based PVT-assisted heat pump water heating (PVTA-HPWH) system, Sol. Energy. 122 (2015) 36–47. doi:10.1016/j.solener.2015.08.024.

[15] A. Del Amo, A. Martínez-Gracia, A.A. Bayod-Rújula, M. Cañada, Performance analysis and experimental validation of a solar-assisted heat pump fed by photovoltaic-thermal collectors, Energy. 169 (2019) 1214–1223. doi:10.1016/j.energy.2018.12.117.

[16] G. Wang, Z. Quan, Y. Zhao, P. Xu, C. Sun, Experimental Study of a Novel PV/T- Air Composite Heat Pump Hot Water System, Energy Procedia. 70 (2015) 537–543. doi:10.1016/j.egypro.2015.02.158.

[17] M. Qu, J. Chen, L. Nie, F. Li, Q. Yu, T. Wang, Experimental study on the operating characteristics of a novel photovoltaic/thermal integrated dual-source heat pump water heating system, Appl. Therm. Eng. 94 (2016) 819–826. doi:10.1016/j.applthermaleng.2015.10.126.

[18] H. Kim, Y. Nam, S. Bae, S. Cho, Study on the Performance of Multiple Sources and Multiple Uses Heat Pump System in Three Different Cities, Energies. 13 (2020) 5211. doi:10.3390/en13195211.

[19] Y. Bai, T.T. Chow, C. Ménézo, P. Dupeyrat, Analysis of a hybrid PV/thermal solar-assisted heat pump system for sports center water heating application, Int. J. Photoenergy. 2012 (2012). doi:10.1155/2012/265838.

[20] M. Izquierdo, P. de Agustín-Camacho, Solar heating by radiant floor: Experimental results and emission reduction obtained with a micro photovoltaic-heat pump system, Appl. Energy. 147 (2015) 297–307. doi:10.1016/j.apenergy.2015.03.007.

[21] J. Yao, H. Xu, Y. Dai, M. Huang, Performance analysis of solar assisted heat pump coupled with build-in PCM heat storage based on PV/T panel, Sol. Energy. 197 (2020) 279–291. doi:10.1016/j.solener.2020.01.002.

[22] X. Zhang, X. Zhao, J. Shen, J. Xu, X. Yu, Dynamic performance of a novel solar photovoltaic/loop-heat-pipe heat pump system, Appl. Energy. 114 (2014) 335–352. doi:10.1016/j.apenergy.2013.09.063.

[23] W. Lerch, A. Heinz, R. Heimrath, Direct use of solar energy as heat source for a heat pump in comparison to a conventional parallel solar air heat pump system, Energy Build. 100 (2015) 34–42. doi:10.1016/j.enbuild.2015.03.006.

[24] J. Zhou, X. Zhao, X. Ma, Z. Qiu, J. Ji, Z. Du, M. Yu, Experimental investigation of a solar driven direct-expansion heat pump system employing the novel PV/micro-channels-evaporator modules, Appl. Energy. 178 (2016) 484–495. doi:10.1016/j.apenergy.2016.06.063.

[25] C. Zhou, R. Liang, J. Zhang, A. Riaz, Experimental study on the cogeneration performance of roll-bond-PVT heat pump system with single stage compression during summer, Appl. Therm. Eng. 149 (2019) 249–261. doi:10.1016/j.applthermaleng.2018.11.120.

[26] Y. Liu, G. Zhoua, J. Ma, Experimental investigation on a solar air heat pump by heat source, Energy Procedia. 14 (2012) 1590–1594. doi:10.1016/j.egypro.2011.12.1137.

[27] X. Zheng, H.Q. Li, M. Yu, G. Li, Q.M. Shang, Benefit analysis of air conditioning systems using multiple energy sources in public buildings, Appl. Therm. Eng. 107 (2016) 709–718. doi:10.1016/j.applthermaleng.2016.04.078.

[28] Y. Qiu, M. Li, R.H.E. Hassanien, Y. Wang, X. Luo, Q. Yu, Performance and operation mode analysis of a heat recovery and thermal storage solar-assisted heat pump drying system, Sol. Energy. 137 (2016) 225–235. doi:10.1016/j.solener.2016.08.016.

[29] J. Zhou, X. Zhao, X. Ma, Z. Du, Y. Fan, Y. Cheng, X. Zhang, Clear-days operational performance of a hybrid experimental space heating system employing the novel mini-channel solar thermal & PV/T panels and a heat pump, Sol. Energy. 155 (2017) 464–477. doi:10.1016/j.solener.2017.06.056.

[30] E. Bellos, C. Tzivanidis, K. Moschos, K.A. Antonopoulos, Energetic and financial evaluation of solar assisted heat pump space heating systems, Energy Convers. Manag. 120 (2016) 306–319. doi:10.1016/j.enconman.2016.05.004.

[31] H.D. Fu, G. Pei, J. Ji, H. Long, T. Zhang, T.T. Chow, Experimental study of a photovoltaic solar-assisted heat-pump/heat-pipe system, Appl. Therm. Eng. 40 (2012) 343–350. doi:10.1016/j.applthermaleng.2012.02.036.

[32] E. Bellos, C. Tzivanidis, Energetic and financial sustainability of solar assisted heat pump heating systems in Europe, Sustain. Cities Soc. 33 (2017) 70–84. doi:10.1016/j.scs.2017.05.020.

[33] Y. Xu, F. Guo, M. Song, N. Jiang, Q. Wang, G. Chen, Exergetic and economic analyses of a novel modified solar-heat-powered ejection-compression refrigeration cycle comparing with conventional cycle, Energy Convers. Manag. 168 (2018) 107–118. doi:10.1016/j.enconman.2018.04.098.

[34] C. Dang, Study on Ejector - Vapor Compression Hybrid Air Conditioning System Using Solar Energy, Int. Refrig. Air Cond. Conf. (2012).

[35] J. Chen, J. Yu, Theoretical analysis on a new direct expansion solar assisted ejector-compression heat pump cycle for water heater, Sol. Energy. 142 (2017) 299–307. doi:10.1016/j.solener.2016.12.043.

[36] X. Wang, Y. Yan, E. Wright, X. Hao, N. Gao, Prospect Evaluation of Low-GWP Refrigerants R1233zd(E) and R1336mzz(Z) Used in Solar-Driven Ejector-Vapor Compression Hybrid Refrigeration System, J. Therm. Sci. 29 (2020).

doi:10.1007/s11630-020-1297-z.

[37] Y. Xu, N. Jiang, Q. Wang, X. Han, Z. Gao, G. Chen, Proposal and thermodynamic analysis of an ejection–compression refrigeration cycle driven by low-grade heat, Energy Convers. Manag. 145 (2017) 343–352. doi:10.1016/j.enconman.2017.05.013.

[38] Y. Xu, C. Wang, N. Jiang, M. Song, Q. Wang, G. Chen, A solar-heat-driven ejector-assisted combined compression cooling system for multistory building – Application potential and effects of floor numbers, Energy Convers. Manag. 195 (2019) 86–98. doi:10.1016/j.enconman.2019.04.090.

[39] R. Law, A. Harvey, D. Reay, Opportunities for low-grade heat recovery in the UK food processing industry, Appl. Therm. Eng. 53 (2013) 188–196. doi:10.1016/j.applthermaleng.2012.03.024.

[40] C.A. Ramírez, M. Patel, K. Blok, From fluid milk to milk powder: Energy use and energy efficiency in the European dairy industry, Energy. 31 (2006) 1984–2004. doi:10.1016/j.energy.2005.10.014.

[41] S. Buffa, M. Cozzini, M. D'Antoni, M. Baratieri, R. Fedrizzi, 5th generation district heating and cooling systems: A review of existing cases in Europe, Renew. Sustain. Energy Rev. 104 (2019) 504–522. doi:10.1016/j.rser.2018.12.059.

[42] Alliance for European Logistics, A Technology Roadmap for Logistics, (2010) 1–12.

[43] P. Byrne, R. Ghoubali, Exergy analysis of heat pumps for simultaneous heating and cooling, Appl. Therm. Eng. 149 (2019) 414–424. doi:10.1016/j.applthermaleng.2018.12.069.

[44] K. Dasi, S. Singh, A.M. Guruchethan, M.P. Maiya, A. Hafner, K. Banasiak, P. Neksa, Performance evaluation of ejector based CO2 system for simultaneous heating and cooling application in an Indian dairy industry, Therm. Sci. Eng. Prog. 20 (2020) 100626. doi:10.1016/j.tsep.2020.100626.

[45] J.M.M. Belman-Flores, A. Mota-Babiloni, S. Ledesma, P. Makhnatch, Using ANNs to approach to the energy performance for a small refrigeration system working with R134a and two alternative lower GWP mixtures, Appl. Therm. Eng. 127 (2017). doi:10.1016/j.applthermaleng.2017.08.108.

[46] P. Makhnatch, A. Mota-Babiloni, A. López-Belchí, R. Khodabandeh, R450A and R513A as lower GWP mixtures for high ambient temperature countries: Experimental comparison with R134a, Energy. 166 (2019) 223–235. doi:10.1016/j.energy.2018.09.001.

[47] M. Yang, H. Zhang, Z. Meng, Y. Qin, Experimental study on R1234yf/R134a mixture (R513A) as R134a replacement in a domestic refrigerator, Appl. Therm. Eng. 146 (2019) 540–547. doi:10.1016/j.applthermaleng.2018.09.122.

[48] J. Sun, W. Li, B. Cui, Energy and exergy analyses of R513a as a R134a drop-in replacement in a vapor compression refrigeration system, Int. J. Refrig. 112 (2020) 348–356. doi:10.1016/j.ijrefrig.2019.12.014.

[49] S.A. Klein, Engineering Equation Solver, (2019).

[50] ASHREA, Standard 34-2016, Designation and Safety Classification of Refrigerants, 2016.

[51] Statistical Office of the European Communities., Energy, transport and environment statistics : 2019 edition, 2019.

[52] W.U. Ground, weather under ground, IBM Weather. (n.d.).

[53] G. Xu, S. Deng, X. Zhang, L. Yang, Y. Zhang, Simulation of a photovoltaic/thermal heat pump system having a modified collector/evaporator, Sol. Energy. 83 (2009) 1967–1976. doi:10.1016/j.solener.2009.07.008.

[54] Y.W. Li, R.Z. Wang, J.Y. Wu, Y.X. Xu, Experimental performance analysis and optimization of a direct expansion solar-assisted heat pump water heater, Energy. 32 (2007) 1361–1374. doi:10.1016/j.energy.2006.11.003.

[55] P. Makhnatch, R. Khodabandeh, The role of environmental metrics (GWP, TEWI, LCCP) in the selection of low GWP refrigerant, Energy Procedia. 61 (2014) 2460–2463. doi:10.1016/j.egypro.2014.12.023.

[56] The European Environment Agency, CO2 emission intensity, (2018).

[57] O. Brunin, M. Feidt, B. Hivet, Comparison of the working domains of some compression heat pumps and a compression-absorption heat pump, Int. J. Refrig. 20 (1997) 308–318. doi:10.1016/S0140-7007(97)00025-X.

[58] B.J. Huang, J.M. Chang, C.P. Wang, V.A. Petrenko, 1-D analysis of ejector performance, Int. J. Refrig. 22 (1999) 354–364. doi:10.1016/S0140-7007(99)00004-3.

[59] J.A. Duffie, W.A. Beckman, J. McGowan, Solar Engineering of Thermal Processes, 1985. doi:10.1119/1.14178.

[60] X. Zhang, X. Zhao, J. Xu, X. Yu, Characterization of a solar photovoltaic/loop-heat-pipe heat pump water heating system, Appl. Energy. 102 (2013) 1229–1245. doi:10.1016/j.apenergy.2012.06.039.

[61] A.K. Shaker Al-Sayyab, Z.Y. Al Tmari, M.K. Taher, Theoretical and experimental investigation of photovoltaic cell performance, with optimum tilted angle: Basra city case study, Case Stud. Therm. Eng. 14 (2019) 100421. doi:10.1016/j.csite.2019.100421.

[62] H. Informed, Danfoss Explains How To Provide Optimal SH For Process Cooling In Food Industry Minimum stable superheat, 2019.

[63] A. Mota-Babiloni, J.R. Barbosa, P. Makhnatch, J.A. Lozano, Assessment of the utilization of equivalent warming impact metrics in refrigeration, air conditioning and heat pump systems, Renew. Sustain. Energy Rev. 129 (2020) 109929. doi:https://doi.org/10.1016/j.rser.2020.109929.